Time-delayed quantum coherent Pyragas feedback control of photon squeezing in a degenerate parametric oscillator

Manuel Kraft,[1,*] Sven M. Hein,[1] Judith Lehnert,[2] Eckehard Schöll,[2] Stephen Hughes,[3] and Andreas Knorr[1]

[1]*Technische Universität Berlin, Institut für Theoretische Physik, Nichtlineare Optik und Quantenelektronik, Hardenbergstraße 36, 10623 Berlin, Germany*

[2]*Technische Universität Berlin, Institut für Theoretische Physik, Nichtlineare Dynamik und Kontrolle, Hardenbergstraße 36, 10623 Berlin, Germany*

[3]*Department of Physics, Engineering Physics and Astronomy, Queen's University, Kingston, Ontario K7L 3N6, Canada*

(Received 24 March 2016; published 1 August 2016)

Quantum coherent feedback control is a measurement-free control method fully preserving quantum coherence. In this paper we show how time-delayed quantum coherent feedback can be used to control the degree of squeezing in the output field of a cavity containing a degenerate parametric oscillator. We focus on the specific situation of Pyragas-type feedback control where time-delayed signals are fed back directly into the quantum system. Our results show how time-delayed feedback can enhance or decrease the degree of squeezing as a function of time delay and feedback strength.

DOI: 10.1103/PhysRevA.94.023806

I. INTRODUCTION

Quantum coherent feedback control [1] has become an increasing field of research in recent years [2]. In contrast to measurement-based quantum control schemes, coherent feedback control does not require quantum state projection by a measurement and therefore fully preserves the quantum coherence. This offers new and interesting possibilities for the control of quantum systems. In particular, coherent time-delayed feedback has been proposed as noninvasive Pyragas-type [3–6] control scenarios [7,8], entanglement control in a quantum node network [9,10], and enhancement of atomic lifetimes by shaping the vacuum [11] or controlling atoms in cavities in front of a mirror [8,12].

Squeezed states of light [13,14] have found important application in a broad area of quantum optics and quantum information processing, providing, for example, an entanglement resource for many quantum information protocols such as quantum key distribution schemes [15] or a signature of quantum synchronization and quantum chimeras [16].

Much work has been done in the control of squeezing of a degenerate parametric oscillator (DPO) in quantum optics. An early attempt [17,18] used a measurement-based feedback scheme to enhance the squeezing of a cavity mode. Recent theoretical research in coherent feedback control introduces a feedback loop through a beam splitter [19,20]. Experimental verification in the instantaneous limit [21] and time-delayed feedback [22] has shown the possibilities but also limitations of coherent control of squeezing. Most of the recent work is done in the instantaneous feedback limit. However, time delays in quantum systems are often unavoidable.

In this paper, we study the squeezing spectrum of the output field of a cavity containing a degenerate parametric oscillator controlled by quantum coherent time-delayed feedback. We focus on the specific situation of Pyragas control, where the difference of instantaneous and time-delayed signal acts as a control force and is fed back into the quantum system [7,23]. Pyragas control has been used in classical systems to stabilize unstable periodic orbits. An advantage is that in the case of stabilization, the control force vanishes, making the control scheme noninvasive. Another characteristic is that no detailed model of the system dynamics has to be known, since it is sufficient to measure an output signal to construct the difference between instantaneous and time-delayed signal.

For our purpose we introduce a quantum mechanical description of time-delayed quantum coherent feedback in the framework of the input-output formalism introduced by Gardiner and Collett [24]. The proposed scheme can be realized in a number of ways, e.g., by a mirror or nanophotonic devices such as photonic crystal waveguides [25–28].

The paper is organized as follows: First, we will introduce our system and feedback scheme and derive the equations of motion for the internal dynamics and the output fields using input-output theory presented in the appendix. Second, to achieve realistic control conditions we will make a stability analysis to obtain the asymptotic behavior of the controlled system. Third, we calculate the squeezing spectrum of the output fields and discuss how the feedback scheme influences the squeezing performance. In the appendix we will show thoroughly that the dynamics of a system coherently interacting with itself through a feedback loop can be represented as a cascaded system, where previous versions of the system drive the present system, leading to time-delayed quantum Langevin equations in the Heisenberg picture [24]. A key advantage of this approach is that it allows physical insight on how feedback coherently returns the out-coupled information back into the system.

II. DEGENERATE PARAMETRIC OSCILLATORS

The degenerate parametric oscillator (DPO) is a well-known nonlinear optical device which allows for squeezing of externally applied light fields. We study the effect of feedback on the steady-state squeezing spectrum of the output fields quadrature phases.

*kraft@itp.tu-berlin.de

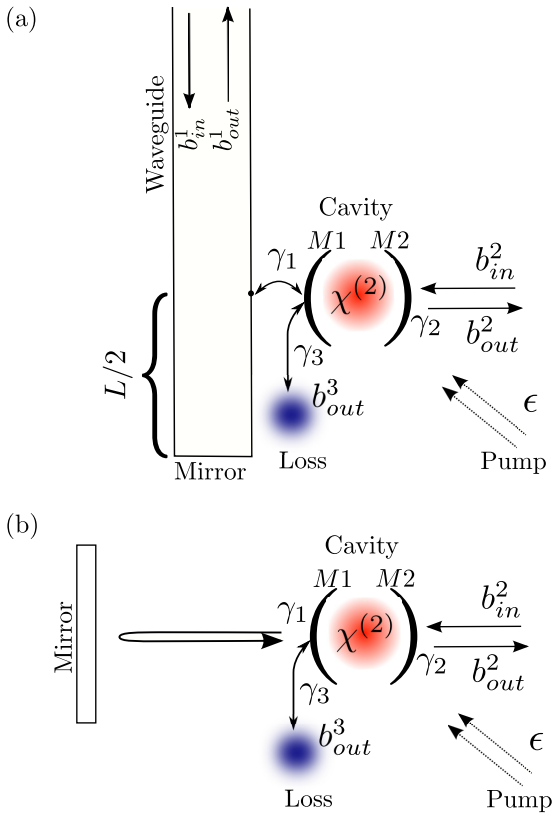

FIG. 1. Schematic of our physical setup and model. A degenerate parametric oscillator (DPO) is embedded in a cavity and driven by a laser with pumping strength $|\epsilon|$. The cavity mirror M_2 with loss rate γ_2 is coupled to an external reservoir denoted by the input b^2_{in} and output b^2_{out}. (a) The mirror M_1 is coupled to a photonic waveguide terminated by a mirror at a distance $L/2$ from the coupling point. The waveguide mirror will introduce a phase shift $\phi = \pi$ for the reflected field and time-delayed feedback into the system. For the case of imperfect coupling to the waveguide, we additionally implement another loss reservoir, graphically denoted by the blue cloud and coupling strength γ_3. (b) Instead of a waveguide, we let the outgoing radiation from M_1 directly emit onto an external mirror.

The DPO, a second-order nonlinear crystal (susceptibility $\chi^{(2)}$), is embedded in a two-sided cavity [29] and externally pumped; see Fig. 1. The cavity mirrors $M1$ and $M2$ are assumed to be lossy with different photon-decay loss rates, but assumed to be transparent at the pump field frequency ω_p [30]. The output field of $M1$ is redirected back to $M1$, becoming a new input. Such a setup will introduce time delay in the equation of motion of the system operator (see below). It can be realized in different ways, with two examples shown in Figs. 1(a) and 1(b).

A. Case (a), feedback from a semi-infinite waveguide [Fig. 1(a)]

The first possibility is to introduce feedback to the DPO at a distance $L/2$ from the end of a semi-infinite waveguide [31]. This setup is schematically shown in Fig. 1(a). Here, the mirror at one end of the waveguide might also be realized by an additional cavity [27]. The internal mode distribution in the waveguide can be modeled by a structured reservoir with a continuum of modes [7,26,32,33]. This will be the setup discussed in this paper.

B. Case (b), feedback from an external mirror [Fig. 1(b)]

However, there are other setups in which time-delayed feedback, and therefore the discussed effects, may appear. For example, the DPO might emit radiation onto a mirror at distance $L/2$, which then projects this radiation back into the DPO with a time delay. Let us therefore briefly consider the DPO emitting directly into modes of an external mirror [12,34,35]; see Fig. 1(b). This setup is often used for semiclassical models of a laser in front of a mirror and is referred to as the Lang-Kobayashi model in laser physics [36,37]. In our case, however, the description is fully quantum mechanical.

In both setups, the emitted signal interacts with the system again after a delay τ, which is why we can model them on equal footing. In the appendix, we show their equivalence (A 3); the difference is that for the first setup [Fig. 1(a)] there are two output fields accessible by measurement (at the waveguide and the mirror $M2$), in contrast to the second setup [Fig. 1(b)], where only the output field from mirror $M2$ is accessible.

Importantly, we consider the realistic case where dissipation is included, i.e., a fraction of the light emitted by the system through the mirror $M1$ couples with strength γ_1 to the structured feedback reservoir, which we introduce via the input operator b^1_{in} [cf. Figs. 1(a) and 1(b)]. The remaining part of radiation which does not interact with the system again is modeled via another Markovian loss through a reservoir described with its input operator b^3_{in}, and the coupling strength of the system is expressed by γ_3. A similar approach considering an atom in front of a mirror is found in Ref. [12]. Moreover, the losses at the second cavity mirror $M2$ are described through the operator b^2_{in} with coupling strength γ_2.

The system Hamiltonian of the pumped DPO is [30]

$$H_{\text{sys}} = \hbar\omega_0 c^\dagger c + \frac{i\hbar}{2}\left(\epsilon e^{-i\omega_p t} c^{\dagger 2} - \epsilon^* e^{i\omega_p t} c^2\right) \tag{1}$$

where

$$\epsilon = |\epsilon| e^{i\Phi} \tag{2}$$

denotes the effective complex valued strength of the pump intensity and is proportional to the second-order nonlinearity $\chi^{(2)}$. The operator c is the photon annihilation operator of the cavity mode. The cavity mode frequency and the laser pump frequency are ω_0 and ω_p, respectively. The inclusion of only one cavity mode in the calculations is a well established approximation [29,30] as long as the combined losses of the cavity are much smaller than the frequency difference between adjacent cavity modes.

The following derivation of the feedback-controlled DPO is in analogy to the seminal work of Collett and Gardiner [29], in which a DPO *without* feedback control is discussed. In particular, in Ref. [29] it is shown that a driven DPO in a cavity can exhibit different squeezing behavior depending on the cavity mirror reflectivities. The effects of time-delayed feedback discussed in this paper can also be interpreted via a frequency-dependent reflectivity of one of the cavity mirrors, as we will show below.

In the appendix, Sec. A 1, it is shown that from (A4) the equation of motion of the operator c subject to time-delayed feedback is

$$\begin{aligned}\dot{c}(t) = &- i\omega_0 c + \epsilon e^{-i\omega_p t} c^\dagger(t) - G c(t) + \gamma_1 c(t-\tau) \\ &- \sqrt{\gamma_1}\, b^1_{\rm in}(t) + \sqrt{\gamma_1}\, b^1_{\rm in}(t-\tau) \\ &- \sqrt{\gamma_2}\, b^2_{\rm in}(t) - \sqrt{\gamma_3}\, b^3_{\rm in}(t),\end{aligned} \tag{3}$$

with $G = (2\gamma_1 + \gamma_2 + \gamma_3)/2$, and the input operators $b^k_{\rm in}(t) = 1/\sqrt{2\pi}\int_{-\infty}^{\infty} d\omega\, b^k_0(\omega) e^{-i\omega t}$, which only depend on the initial reservoir operator $b^k_{t=0}(\omega)$ $(k = 1,2,3)$.

We have set the phase-shift ϕ introduced by the mirror in the feedback loop in (A4) to $\phi = \pi$ [cf. Fig. 1]. We neglect here any frequency dependence of the phase shift within the waveguide. Moreover, we consider that no losses occur for the fields when reflected by the external mirror. This is modeled by choosing $\gamma_f = \gamma_1$ in Eq. (A4). The delay τ is the time needed by the field emitted at $M1$ to return back to $M1$; therefore $\tau = L/c_0$ with $L/2$ being the system-mirror distance and c_0 being the speed of light in the vacuum or in the waveguide.

At this point, it is interesting to compare the delay times τ to the round trip time $\tau_{\rm cav}$ *within* the cavity containing the nonlinear medium. As we pointed out above, we need the cavity mode separation $\delta\omega_0$ to be much larger than the loss rate G of the cavity: $\delta\omega_0 \gg G$. The cavity round trip time $\tau_{\rm cav}$ is directly related to the mode separation via $\tau_{\rm cav} = 2\pi/(\delta\omega_0)$. For feedback delay times comparable with G^{-1}, this leads to the condition $\tau_{\rm cav} \ll \tau$. This means that our analysis is especially suited for small DPO cavities, e.g., in microcavity-based implementations [38,39].

We choose the pump frequency ω_p to be $2\omega_0$ and move to a rotating frame of frequency ω_0. In the rotating frame, the equations become in matrix form

$$\begin{aligned}\dot{\mathbf{c}}(t) = &\,\overline{\mathbf{A}}\mathbf{c}(t) + \gamma_1 \overline{\mathbf{B}}\mathbf{c}(t-\tau) \\ &- \sqrt{\gamma_1}\, \mathbf{b}^1_{\rm in}(t) + \sqrt{\gamma_1}\, \overline{\mathbf{B}}\mathbf{b}^1_{\rm in}(t-\tau) \\ &- \sqrt{\gamma_2}\, \mathbf{b}^2_{\rm in}(t) - \sqrt{\gamma_3}\, \mathbf{b}^3_{\rm in}(t),\end{aligned} \tag{4}$$

where

$$\overline{\mathbf{A}} = \begin{pmatrix} -G & \epsilon \\ \epsilon^* & -G \end{pmatrix} \quad \text{and} \quad \overline{\mathbf{B}} = \begin{pmatrix} e^{i\omega_0\tau} & 0 \\ 0 & e^{-i\omega_0\tau} \end{pmatrix} \tag{5}$$

and using the operator vector notation,

$$\mathbf{c}(t) = \begin{pmatrix} c(t) \\ c^\dagger(t) \end{pmatrix} \quad \text{and} \quad \mathbf{b}^k_{\rm in}(t) = \begin{pmatrix} b^k_{\rm in}(t) \\ b^{k\dagger}_{\rm in}(t) \end{pmatrix}, \tag{6}$$

with $k \in \{1,2,3\}$. Note that due to the transformation to the rotating frame, the matrix $\overline{\mathbf{A}}$ has no dependence on ω_0.

Since Eq. (4) is linear, we can solve it using Fourier transform techniques. We define the Fourier transform of an arbitrary field operator $O(t)$ as

$$\tilde{O}(w) = \frac{1}{\sqrt{2\pi}} \int_{-\infty}^{\infty} dt\, e^{-i\omega t} O(t). \tag{7}$$

Note that

$$[\tilde{O}(\omega)]^\dagger = \left[\frac{1}{\sqrt{2\pi}} \int_{-\infty}^{\infty} dt\, e^{-i\omega t} O(t)\right]^\dagger = \tilde{O}^\dagger(-\omega) \tag{8}$$

so that $\tilde{\mathbf{O}}(\omega) = \begin{pmatrix} \tilde{O}(\omega) \\ \tilde{O}^\dagger(-\omega) \end{pmatrix}$.

The solution to Eq. (4) reads

$$\begin{aligned}\tilde{\mathbf{c}}(w) = \overline{\mathbf{M}}^{-1}\Bigg[&-\sqrt{\gamma_1}\begin{pmatrix} s(\omega) & 0 \\ 0 & s^*(-\omega) \end{pmatrix} \tilde{\mathbf{b}}^1_{\rm in}(w) \\ &- \sqrt{\gamma_2}\tilde{\mathbf{b}}^2_{\rm in}(\omega) - \sqrt{\gamma_3}\tilde{\mathbf{b}}^3_{\rm in}(\omega)\Bigg],\end{aligned} \tag{9}$$

where $s(\omega)$ and $\overline{\mathbf{M}}$ are given by

$$s(\omega) = 1 - e^{-i(\omega-\omega_0)\tau}, \tag{10}$$

$$\overline{\mathbf{M}} = \begin{pmatrix} i\omega + \frac{\gamma_2+\gamma_3}{2} + \gamma_1 s(\omega) & -\epsilon \\ -\epsilon^* & i\omega + \frac{\gamma_2+\gamma_3}{2} + \gamma_1 s^*(-\omega) \end{pmatrix}. \tag{11}$$

The function $s(\omega)$ describes a frequency dependence of the loss through the channel described by γ_1. As it appears both in the matrix $\overline{\mathbf{M}}$ and as the coupling strength for the field $b^1_{\rm in}$, we can already expect important frequency-dependent features in the squeezing spectra. We introduce Z as an abbreviation for the matrix elements of $\overline{\mathbf{M}}$: $\overline{\mathbf{M}} \equiv \begin{pmatrix} Z(\omega) & -\epsilon \\ -\epsilon^* & Z^*(-\omega) \end{pmatrix}$.

After inverting $\overline{\mathbf{M}}$ we find for the internal cavity mode

$$\begin{aligned}\tilde{c}(\omega) = &\,\mathcal{A}^-_1(\omega)\tilde{b}^1_{\rm in}(\omega) + \mathcal{A}^+_1(\omega)\tilde{b}^{1\dagger}_{\rm in}(-\omega) \\ &+ \mathcal{A}^-_2(\omega)\tilde{b}^2_{\rm in}(\omega) + \mathcal{A}^+_2(\omega)\tilde{b}^{2\dagger}_{\rm in}(-\omega) \\ &+ \mathcal{A}^-_3(\omega)\tilde{b}^3_{\rm in}(\omega) + \mathcal{A}^+_3(\omega)\tilde{b}^{3\dagger}_{\rm in}(-\omega),\end{aligned} \tag{12}$$

with

$$\begin{aligned}\mathcal{A}^-_1(\omega) &= \frac{-\sqrt{\gamma_1}s(\omega)Z^*(-\omega)}{\Delta(\omega)}, & \mathcal{A}^+_1(\omega) &= \frac{-\sqrt{\gamma_1}s^*(-\omega)\epsilon}{\Delta(\omega)}, \\ \mathcal{A}^-_2(\omega) &= \frac{-\sqrt{\gamma_2}Z^*(-\omega)}{\Delta(\omega)}, & \mathcal{A}^+_2(\omega) &= \frac{-\sqrt{\gamma_2}\epsilon}{\Delta(\omega)}, \\ \mathcal{A}^-_3(\omega) &= \frac{-\sqrt{\gamma_3}Z^*(-\omega)}{\Delta(\omega)}, & \mathcal{A}^+_3(\omega) &= \frac{-\sqrt{\gamma_3}\epsilon}{\Delta(\omega)},\end{aligned} \tag{13}$$

where

$$\Delta(\omega) = \det(\overline{\mathbf{M}}) = Z(\omega)Z^*(-\omega) - |\epsilon|^2. \tag{14}$$

Equation (12) describes the internal field dynamics, provided the input fields are known. The next step is to calculate the output fields, since these determine the squeezing spectrum in an experiment [22].

III. THE OUTPUT FIELDS

So far we have determined the dynamics of the internal mode in terms of the input fields. The output is determined by the input-output relations (A5) and (A10) and relies on the input fields from mirror and waveguide, respectively. There are two detectable output fields, $b^1_{\rm out}$ and $b^2_{\rm out}$, accessible by measurement in the case covered by Fig. 1(a). However, when the feedback is realized by a mirror [Fig. 1(b)], the input and output fields $b^1_{\rm in/out}$ cannot be accessed by measurement in a straightforward way. They model the reservoir in which the so-called in-loop excitation is lost after one round trip. In that case, only $b^2_{\rm out}$ can be measured.

In the appendix (Sec. A 4) it is shown that in frequency space, the output fields take the general form

$$\tilde{b}^i_{\rm out}(\omega) = X_i(\omega)\tilde{b}^i_{\rm in}(\omega) + Y_i(\omega)\tilde{c}(\omega). \tag{15}$$

where X_i and Y_i are defined in Eq. (A14).

For the direct input-output connection at $M2$ we simply have $X_2 = 1$ and $Y_2 = \sqrt{\gamma_2}$ reducing the above expression to the standard input-output relation $\tilde{b}^2_{\rm out}(\omega) = \tilde{b}^2_{\rm in}(\omega) + \sqrt{\gamma_2}\tilde{c}(\omega)$ [30]. At the waveguide output, Eq. (A10) applies. We find after transformation in the rotating frame and in frequency space $X_1(\omega) = -e^{-i(\omega-\omega_0)\tau}$ and $Y_1(\omega) = \sqrt{\gamma_1} - \sqrt{\gamma_1}e^{-i(\omega-\omega_0)\tau} = \sqrt{\gamma_1}s(\omega)$.

The relation (15) can be rewritten with (12) as

$$\tilde{b}^i_{\rm out}(\omega) = \sum_j \mathcal{S}^-_{ij}(\omega)\tilde{b}^j_{\rm in}(\omega) \tag{16}$$

$$+ \sum_j \mathcal{S}^+_{ij}(\omega)\tilde{b}^{j\dagger}_{\rm in}(-\omega), \tag{17}$$

where

$$\mathcal{S}^-_{ij}(\omega) = Y_i(\omega)\mathcal{A}^-_j(\omega) + X_i(\omega)\delta_{ij}, \tag{18}$$

$$\mathcal{S}^+_{ij}(\omega) = Y_i(\omega)\mathcal{A}^+_j(\omega). \tag{19}$$

So far we have algebraically eliminated the in-loop field and the internal mode by re-expressing the output fields in terms of the input fields. That was straightforward since the equations are linear in frequency space. Similar approaches in linear quantum networks are found in Refs. [19,20]. Identifying X_i and Y_i from expression (15) allows us to compute $\mathcal{S}^{\mp}_{ij}$.

Given that the input fields are in the vacuum state, only antinormally ordered correlations are nonvanishing, that is,

$$\left\langle \tilde{b}^i_{\rm in}(\omega)\tilde{b}^{j\dagger}_{\rm in}(-\omega')\right\rangle = \delta_{ij}\delta(\omega+\omega'), \tag{20}$$

and all other correlations of the input fields are zero.

In this case we find for the reservoir output fields

$$\left\langle \tilde{b}^i_{\rm out}(\omega)\tilde{b}^{i\dagger}_{\rm out}(-\omega')\right\rangle = \mathcal{N}_i(\omega)\delta(\omega+\omega'),$$
$$\left\langle \tilde{b}^i_{\rm out}(\omega)\tilde{b}^{i}_{\rm out}(\omega')\right\rangle = \mathcal{M}_i(\omega)\delta(\omega+\omega'), \tag{21}$$

where

$$\mathcal{N}_i(\omega) = \sum_j |\mathcal{S}^-_{ij}(\omega)|^2,$$

$$\mathcal{M}_i(\omega) = \sum_j \mathcal{S}^-_{ij}(\omega)\mathcal{S}^+_{ij}(-\omega), \tag{22}$$

where $\mathcal{S}^{\pm}_{ij}$ are defined in Eqs. (18) and (19).

Furthermore we have the identity

$$\sum_j |\mathcal{S}^-_{ij}(\omega)|^2 - |\mathcal{S}^+_{ij}(\omega)|^2 = 1. \tag{23}$$

This ensures that the output fields satisfy the usual bosonic commutator relation. Considering the single-input case ($b^1_{\rm in} = 0$ or $b^2_{\rm in} = 0$) this relation simplifies to $|\mathcal{S}^-_{ii}(\omega)|^2 - |\mathcal{S}^+_{ii}(\omega)|^2 = 1$. Then the output is simply a Bogoliubov transformation of the input [19,20].

The system described by Eq. (4) is an open linear system. Energy is not conserved since there are loss and pump channels. We therefore need to analyze whether the system equilibrates at finite values; otherwise, a static analysis for $t \to \infty$ is not reliable. To do so we carry out a stability analysis in the next section.

IV. STABILITY ANALYSIS

Asymptotic stability requires that *all* the roots s of the characteristic equation of Eq. (4),

$$\det[s\mathbf{1} - \overline{\mathbf{A}} - \gamma_1\overline{\mathbf{B}}e^{-\tau s}] = 0, \tag{24}$$

lie in the complex open left half-plane [40,41]. Since the transcendental equation (24) is difficult to solve, we use both a method using the Lambert W function and an analytical treatment for delay-independent stability based on the Routh-Hurwitz criterion [40] to determine the asymptotic stability of our system.

We can dramatically reduce the complexity of the stability analysis by restricting the treatment to two important special cases where the coherent part of the field $b^1_{\rm out,1}(t)$ and the time-delayed and phase shifted in-loop field $-b^1_{\rm out,1}(t-\tau)$ are constructively or destructively interfering at the edge of mirror $M1$. We obtain constructive interference when the condition

$$\omega_0\tau = (2n-1)\pi \tag{25}$$

is matched and destructive interferences for

$$\omega_0\tau = 2n\pi, \tag{26}$$

where $n \in \mathbb{N}$ is any natural number. In the following we restrict the stability analysis to these two cases.

We express the stability condition using a Lambert W function approach. For the two special cases (25) and (26), the characteristic equation (24) can be factorized into the form $(s-\alpha_1-\beta e^{-\tau s})(s-\alpha_2-\beta e^{-\tau s}) = 0$ with $\alpha_1 = |\epsilon| - G$, $\alpha_2 = -|\epsilon| - G$, and $\beta = \pm\gamma_1$, where $+$ results from the condition $\omega_0\tau = 2n\pi$ and $-$ results from $\omega_0\tau = (2n-1)\pi$.

In this case the complex roots of Eq. (24) are given by

$$s_i = \frac{1}{\tau}W_0(\tau\beta e^{-\tau\alpha_i}) + \alpha_i, \quad i = 1,2, \tag{27}$$

where W_0 is the principal branch of the Lambert W function [42,43].

It follows that the system described by Eq. (4) is stable if and only if [41]

$$S^i_W(\alpha_i,\beta,\tau) := \mathrm{Re}[s_i] < 0, \quad i = 1,2. \tag{28}$$

We found that $S^1_W \geqslant S^2_W$, and it is therefore sufficient to consider only S^1_W. Furthermore we can express S^1_W in terms of dimensionless parameters as

$$S^1_W = \frac{1}{\tau}\mathrm{Re}[W_0(\pm\gamma_1\tau e^{\pm\gamma_1\tau(\tilde{\alpha}-1)}) + (\tilde{\alpha}-1)], \tag{29}$$

where again $+$ or $-$ result from the conditions (26) and (25), respectively, and

$$\tilde{\alpha} = \frac{|\epsilon| - (\gamma_2+\gamma_3)/2}{\gamma_1}. \tag{30}$$

This term represents the difference between the pump strength $|\epsilon|$ and losses γ_2 and γ_3 normalized by the feedback strength γ_1.

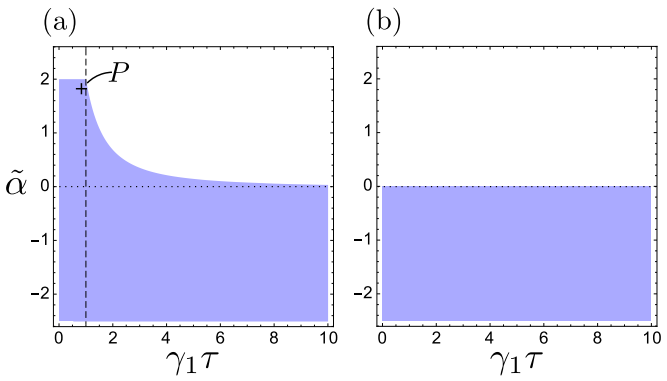

FIG. 2. Stability analysis in the case of constructive (a) and destructive (b) interference as a function of $\gamma_1\tau$ and the effective pump strength $\tilde{\alpha} = [|\epsilon| - 0.5(\gamma_2+\gamma_3)]/\gamma_1$, Eq. (30). The stable regions are the blue (shaded) ones, where $S_W^1 < 0$. (a) Constructive interference $[\omega_0\tau = (2n-1)\pi]$. The boundary line between the stable and unstable region is first constant with $\tilde{\alpha} = 2$ for $\gamma_1\tau < 1$. At $\gamma_1\tau = 1$ there is a stability change. From that point, the stability boundary decreases with growing $\gamma_1\tau > 1$ toward $\tilde{\alpha} \to 0$. This means that for longer delays the stability becomes independent of the coupling γ_1 and of the delay time τ. We call the region where $\gamma_1\tau < 1$ the *short-delay regime* and the region $\gamma_1\tau > 1$ the *long-delay regime*. The dashed line marks the boundary between the short and long feedback regions. The point P represents a fixed value of $|\epsilon| - (\gamma_2+\gamma_3)/2$, which is investigated in Fig. 4. (b) Destructive interference $[\omega_0\tau = (2n-1)\pi]$. The dotted line marks the stability boundary given by Eq. (33), below which the system is guaranteed to be stable independent of delayed feedback effects. We observe that as long $\tilde{\alpha} < 0$, i.e., $|\epsilon| < (\gamma_2+\gamma_3)/2$, the system is stable.

We plot S_W^1 in dependence of the dimensionless parameters $\gamma_1\tau$ and $\tilde{\alpha}$. The results for constructive and destructive interference are shown in Figs. 2(a) and 2(b), respectively.

A. Constructive interference, Fig. 2(a)

We find that the stability region is dependent on $\gamma_1\tau$ and the parameter $\tilde{\alpha}$. For $\gamma_1\tau < 1$, the boundary line between unstable and stable regions is constant with $\tilde{\alpha} = 2$, corresponding to a pump strength $|\epsilon| = 2\gamma_1 + (\gamma_2+\gamma_3)/2$.

For $\gamma_1\tau > 1$ there is a stability change, and the boundary line between unstable and stable region decreases slowly with $\gamma_1\tau$. For sufficiently large $\gamma_1\tau$ the boundary line approaches $\tilde{\alpha} \to 0$, i.e., $|\epsilon| \to (\gamma_2+\gamma_3)/2$. The stability then becomes independent of the coupling to the feedback reservoir and the delay time τ.

We use this boundary line to define what we call the *short-* and the *long-delay regime*: We define the short-delay regime for feedback times and strengths satisfying

$$\gamma_1\tau < 1, \tag{31}$$

and for the long-delay regime

$$\gamma_1\tau > 1. \tag{32}$$

B. Destructive interference, Fig. 2(b)

In the case of destructive interference, we find that the system is stable for all $\gamma_1\tau$ whenever $\tilde{\alpha} < 0$, i.e., $|\epsilon| < (\gamma_2+\gamma_3)/2$. The stability is independent of the coupling to the feedback reservoir and of the delay time.

Using a fully analytical method we can also give a lower limit where the system remains stable independently of the delay time τ. From the Routh-Hurwitz criterion [40] it follows that the system (3) is asymptotically stable over the whole range of possible delays τ if and only if the two following conditions are fulfilled:

(1) The matrix $\overline{\mathbf{A}} + \gamma_1\overline{\mathbf{B}}$ is of Hurwitz type

(2) The auxiliary equation $\det[s\mathbf{1} - \overline{\mathbf{A}} - \gamma_1\overline{\mathbf{B}}(\frac{1-Ts}{1+Ts})^2] = 0$ has no roots on the imaginary axis for any $T \geqslant 0$.

For both cases we find analytically that stability is guaranteed *for all delays* τ [as long as Eqs. (25) or (26) hold] as long as

$$\frac{\gamma_2+\gamma_3}{2} > |\epsilon|. \tag{33}$$

In the case of destructive interference [Eq. (26)] the system is stable if and only if Eq. (33) is fulfilled. In contrast, for constructive interference [Eq. (25)] our analysis above [cf. Fig. 2(a)] shows that there can be stable regions in which Eq. (33) is not fulfilled. For long delays τ, however, Eq. (33) is recovered. In particular, this means that the threshold between stable and unstable behavior will always lie in the area of $\tilde{\alpha} \geqslant 0$. The stability condition given in Eq. (33) is independent of γ_1 and therefore the same as if there was no out-coupling via the feedback channel, i.e., $\gamma_1 = 0$. This means that at least in the two cases of destructive and constructive interference the presence of a channel with time-delayed feedback ($\gamma_1 \neq 0$) can only make the system more stable, but never destabilizes it.

In summary, we find that the DPO losses dissipated into nonfeedback reservoirs must be greater than the pump for the system to be stable. For constructive interference there exist additional losses created by the feedback, which are particularly dominant in the short feedback range $\gamma_1\tau < 1$ as depicted in Fig. 2(a). For destructive interference only nonfeedback terms contribute.

V. SQUEEZING SPECTRUM

We define observables called the output quadratures in Fourier space by [19]

$$\mathbf{X}^i_{\text{out}}(\omega,\theta) = e^{-i\theta}\mathbf{b}^i_{\text{out}}(\omega) + e^{i\theta}\mathbf{b}^{i\dagger}_{\text{out}}(-\omega), \tag{34}$$

for fixed phases θ. We calculate the variance of the quadratures at the output i as

$$\left\langle \mathbf{X}^i_{\text{out}}(\omega,\theta), \mathbf{X}^i_{\text{out}}(\omega',\theta)\right\rangle = \mathcal{P}_i(\omega,\theta)\delta(\omega+\omega'), \tag{35}$$

where $\langle a,b\rangle = \langle ab\rangle - \langle a\rangle\langle b\rangle$ denotes the variance, where $\langle \mathbf{X}^i_{\text{out}}(\omega,\theta)\rangle = 0$, since the quadrature is simply a linear combination of the input fields which are in the vacuum state.

The power spectral density $\mathcal{P}_i$ is referred to as the squeezing spectrum [19,21] and takes the form [cf. Eq. (21)]

$$\mathcal{P}_i(\omega,\theta) = 2\,\text{Re}[e^{-i2\theta}\mathcal{M}_i(\omega)] + \mathcal{N}_i(\omega) + \mathcal{N}_i(-\omega) - 1, \tag{36}$$

with $\mathcal{M}_i$ and $\mathcal{N}_i$ as defined in Eq. (22).

In particular for an (*un*squeezed) coherent state or an (*un*squeezed) vacuum state the variance in the quadratures, Eq. (34), is equal to 1. This limit is referred to as the quantum noise limit. In contrast, a squeezed state is a nonclassical state

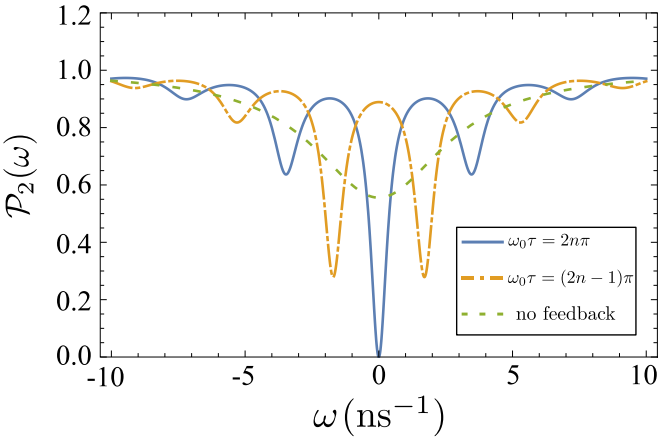

FIG. 3. Long-delay regime. Maximal squeezing spectra (in a frame rotating with ω_0) at the $M2$ output with and without feedback at threshold (in the feedback case) $|\epsilon| = \gamma_2/2$ in the cases $\omega_0\tau = 2n\pi$ and $\omega_0\tau = (2n-1)\pi$ for $\tau \neq 0$. The parameters are $S = 0.5$, $\gamma_1 = \gamma_2 = 2\,\mathrm{ns}^{-1}$, $|\epsilon| = 1\,\mathrm{ns}^{-1}$, and $\gamma_3 = 0$ (ideal feedback coupling). The spectrum is highly structured as a function of ω and τ. For the case of destructive interference ($\omega_0\tau = 2n\pi$) maximal squeezing is achievable at threshold at the central frequency ω_0 ($\omega = 0$ in the plots). On the other hand, constructive interference cannot enhance the squeezing at ω_0. The side peaks show that the feedback scheme shifts the frequencies where squeezing occurs; however, it is never maximal for other frequencies than ω_0. The case without feedback corresponds to a double-sided lossy cavity as discussed in Ref. [29] with respective loss rates $\gamma_1 = \gamma_2 = 2\,\mathrm{ns}^{-1}$ pumped below threshold at $|\epsilon| = 1\,\mathrm{ns}^{-1}$.

of light with the characteristic that for a certain phase θ the variance goes *below* the quantum noise limit.

VI. RESULTS

To understand the delay dependence of the spectrum it is instructive to look at the expression (10) and the matrix (11). The term $s(\omega)$ represents a frequency dependence of the loss through the channel described by γ_1. Compared to the uncontrolled scenario, it will cause a frequency-dependent self-energy of the spectrum. We expect that the Lorentzian form of the spectrum for the uncontrolled system becomes multipeaked, depending on the phase of the in-loop field. Since the influence of $s(\omega)$ scales with the feedback strength γ_1, the frequency-dependent effects increase with growing γ_1. We will proceed to analyze this behavior for different parameters.

For the numerical evaluation we choose the parameters $2\theta = \Phi + \pi$ with $\Phi = \arg(\epsilon)$ [cf. Eq. (2)], $\omega_0 = 1\,\mathrm{fs}^{-1}$ and

$$\tau = (S + 10^{-6}\delta)\pi\ \mathrm{ns}. \tag{37}$$

Here, we divide τ into two contributions: First, the scaling parameter S determines the length of the feedback time in π ns and is chosen such that $S\omega_0$ ns is a natural number. Second, the tuning parameter $\delta \in \{0,1\}$ is such that either the condition $\omega_0\tau = (2n-1)\pi$ (destructive interference) or $\omega_0\tau = 2n\pi$ (constructive interference) is fulfilled. We do focus on these two regimes of destructive and constructive interference to study the highest and lowest possible squeezing performance.

In the following the scaling parameter S is within $\{0.1, 0.5\}$ so that the system-mirror distances (see Fig. 1) are in the range of few centimeters.

The other parameters $|\epsilon|$ (pump), γ_1 (feedback coupling), and $\gamma_{2/3}$ (loss) are varied to address the experimental feasibility of the following numerical results. In the following plots the quantum noise limit is equal to 1. Whenever the values of the spectrum get below the quantum noise limit we have a squeezed quadrature. Perfect squeezing, i.e., maximal noise reduction, is obtained when the variance in the quadrature is zero.

To obtain a detailed analysis of the spectrum at the two output channels b^1_{out} and b^2_{out} we will investigate them for two different parameter sets, representing short- and long-delay times, defined in Eqs. (31) and (32) as $\gamma_1\tau < 1$ and $\gamma_1\tau > 1$, respectively. For each output, we will start with the analysis of long-delay times, where we will find strongly frequency-modulated squeezing spectra. Second, we will investigate the short-delay regime for parameters at which time-delayed feedback is crucial for the stabilization of the system. The results are plotted in Figs. 3–5: Figure 3 shows the spectrum for *long*-delay times at the mirror $M2$, Fig. 4 shows the spectrum for *short*-delay times at the mirror $M2$ as well as

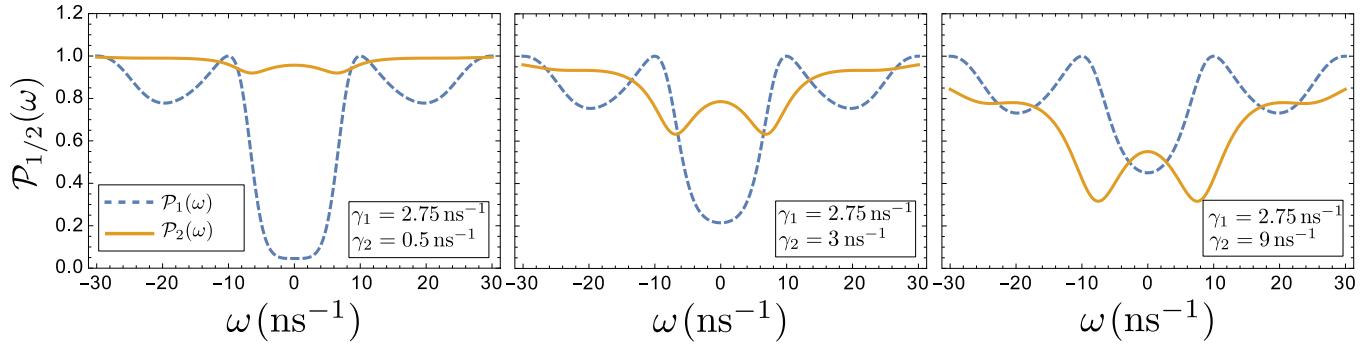

FIG. 4. Short-delay regime. Comparison of the squeezing spectra $\mathcal{P}_1$ and $\mathcal{P}_2$ (in a frame rotating with ω_0) in the case of constructive interference, i.e., $\omega_0\tau = (2n-1)\pi$ for $\tau \neq 0$. The parameters are $S = 0.1$, $\gamma_1 = 2.75\,\mathrm{ns}^{-1}$, $\gamma_2 \in \{0.5, 3, 9\}\,\mathrm{ns}^{-1}$, and a fixed loss-pump strength $|\epsilon| - \gamma_2/2 = 5\,\mathrm{ns}^{-1}$. The situation corresponds to the stable point denoted by P_1 in Fig. 2(a). We see that while γ_2 increases, the squeezing in the output of the waveguide is diminished, whereas the squeezing at the mirror $M2$ output is enhanced. Note that for the present parameters the uncontrolled case ($\gamma_1 = 0$) is not stable and therefore cannot be shown (stability would require $|\epsilon| < \gamma_2/2$).

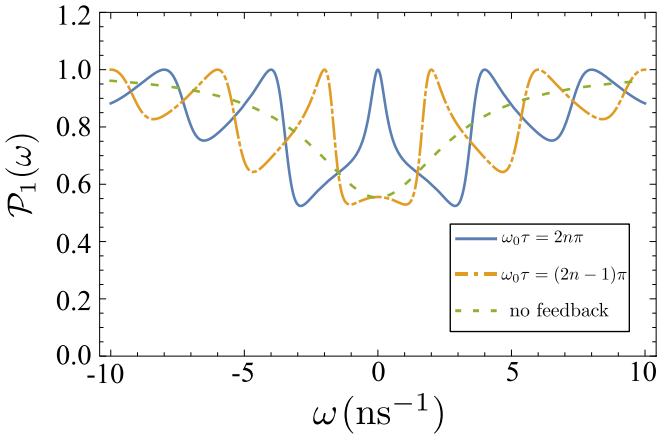

FIG. 5. Long-delay regime. Maximal squeezing spectra (in a frame rotating with ω_0) at the waveguide output with and without feedback at threshold $|\epsilon| = \gamma_2/2$ in the cases $\omega_0\tau = 2n\pi$ and $\omega_0\tau = (2n-1)\pi$ for $\tau \neq 0$. The parameters are $S = 0.5$, $\gamma_1 = \gamma_2 = 2\,\mathrm{ns}^{-1}$, $|\epsilon| = 1\,\mathrm{ns}^{-1}$, and $\gamma_3 = 0$ (ideal feedback coupling). The spectrum is highly structured as a function of ω and τ. For the case of destructive interference ($\omega_0\tau = 2n\pi$) only noise remains as an output at threshold at the central frequency ω_0 ($\omega = 0$ in the plots), and thus $\mathcal{P}_1(\omega_0) = 1$ corresponding to the quantum noise limit and no squeezing is achieved. On the other hand, for constructive interference we observe squeezing of the output field at ω_0. However, for long delays τ in both cases $\gamma_2/2 > |\epsilon|$ is required for stability, which decreases squeezing below 50%. For comparison, the green dashed line marks the squeezing spectrum for the case in which the feedback channel is replaced by a Markovian reservoir with loss rates $\gamma_1 = \gamma_2 = 2\,\mathrm{ns}^{-1}$ pumped below threshold at $|\epsilon| = 1\,\mathrm{ns}^{-1}$.

at the waveguide output, and Fig. 5 shows the spectrum for *long* feedback delay at the waveguide output.

A. Output spectrum at b^2_{out}

In this section, we discuss the squeezing spectrum for the output channel located at mirror $M2$, i.e., b^2_{out}.

1. Long-delay regime

First, we consider ideal feedback ($\gamma_3 = 0$) in the long-delay regime. Nonideal feedback ($\gamma_3 \neq 0$) is discussed further below. Because of the parameter set in this case, we are able to discuss both constructive interference, i.e., condition (25), and destructive interference, i.e., condition (26), at mirror $M1$. The stability analysis, Sec. IV, shows that the system is stable for $|\epsilon| < \gamma_2/2$ over the whole range of τ values, if Eqs. (25) or (26) are fulfilled. The used parameters are $S = 0.5$ and $\gamma_1 = \gamma_2 = 2\,\mathrm{ns}^{-1}$. We evaluate the squeezing spectrum $\mathcal{P}_2$ at the threshold value $|\epsilon| \to \gamma_2/2$. The spectrum is shown in Fig. 3. For comparison, we also plot the spectrum for a system in which the feedback decay channel is replaced by a Markovian reservoir (dashed line). In contrast to the free evolving spectrum without feedback, we observe that the spectrum is highly structured as a function of ω. The frequency modulation is on the order of $O(\pi/\tau)$, and therefore we observe that for longer delays the number of peaks increases within the frequency bandwidth. For long delays, the peak separation can be well approximated by $2\pi/\tau$, while for shorter delays the overall Lorentzian envelope of the spectrum additionally modifies the peak separation. In particular, we find a strong enhancement of squeezing for specific frequencies ω compared to the uncontrolled case. Most importantly, for the case of destructive interference ($\omega_0\tau = 2n\pi$) maximal squeezing ($\mathcal{P}_2 = 0$) is attained at threshold at the central frequency $\omega = \omega_0$ ($\omega = 0$ in the rotating frame in Fig. 3). Here, because of the destructive interference, the feedback channel is closed so that effectively the system behaves like a single-ended cavity [29,44]. The case of constructive interference ($\omega_0\tau = (2n-1)\pi$) shows a good squeezing performance for the first side peaks, whereas no noise reduction is observed at ω_0.

2. Short-delay regime

Let us now reduce the delay time such that $\gamma_1\tau < 1$. We will analyze the system for parameters where time-delayed feedback with *constructive* interference [condition (25)] is crucial for the stability of the system. In particular, we will use the parameters marked as P in Fig. 2(a). We set the delay scaling parameter S [Eq. (37)] to be 0.1 and analyze the squeezing properties for a set of fixed loss-pump differences $|\epsilon| - \gamma_2/2 = 5\,\mathrm{ns}^{-1}$, in which we vary $\gamma_2 \in \{0.5, 3, 9\}\,\mathrm{ns}^{-1}$ and choose the feedback coupling strength to be $\gamma_1 = 2.75\,\mathrm{ns}^{-1}$, which corresponds to $\gamma_1\tau \simeq 0.864$. Again we put $\gamma_3 = 0$ for simplicity. We can only discuss the case for constructive interference, since destructive interference as well as no feedback at all would make the system unstable. The calculated spectra (short delay, constructive interference) are shown in Fig. 4 (solid line). We observe again that the spectrum $\mathcal{P}_2$ is structured as a function of ω, with two main side peaks. We find that while γ_2 increases the squeezing at the mirror $M2$ output is enhanced, but the qualitative behavior does not change. However, it can only be maximal ($\mathcal{P}_2 \to 0$) in the limit situation $\gamma_2 \to \infty$ (not shown). In this case the feedback mechanism can be neglected compared to the losses occurring at the mirror $M2$ output. Below we will analyze the waveguide output spectrum b^1_{out} for the same parameters to get a direct comparison with b^2_{out}. For both cases, i.e., long and short feedback times, we have also investigated the case $\gamma_3 \neq 0$ (not shown). The only effect of $\gamma_3 \neq 0$ is to reduce the squeezing in the spectra, while it does not change the qualitative frequency behavior.

B. Output spectrum at b^1_{out}

Next we address the question of whether the output spectrum depends on the channel of observation, b^1_{out} or b^2_{out}; cf. Fig. 1. For this we discuss the waveguide signal, Fig. 1(a).

1. Long-delay regime

For the discussion of the long-delay situation we evaluate the squeezing spectrum of the b^1_{out} for the same set of parameters as in the long-delay analysis of the b^2_{out} output spectrum. The spectrum is shown in Fig. 5. In the case of long delays for both cases of destructive and constructive interference, $\gamma_2/2 > |\epsilon|$ is required for stability, which decreases squeezing below 50%. In the case of destructive interference we observe $\mathcal{P}_1 = 1$ at the central frequency $\omega = \omega_0$ ($\omega = 0$ in the rotating

frame). In this case only vacuum noise remains at the output of the waveguide, since all the radiation from the cavity is canceled out by its time-delayed counterpart. For comparison, we again also plot the squeezing spectrum *without* feedback, i.e., when replacing the feedback channel by a Markovian reservoir.

2. *Short-delay regime*

We first discuss the spectrum at the output of the waveguide in the short feedback regime in the case of constructive interference, i.e., condition (25) for the same set of parameters as in the short-delay analysis of the b^2_{out} output spectrum. The spectra are shown in Fig. 4 (dashed line). Similar to the b^2_{out} spectrum, the spectra are highly structured as a function of ω with one main peak at the central frequency $\omega = \omega_0$ ($\omega = 0$ in the rotating frame) and two side peaks. We find that for small γ_2 values, i.e., small losses at the mirror $M2$, the squeezing in the b^1_{out} output at the central frequency ω_0 is very high ($\mathcal{P}_1 \to 0$ for $\gamma_2 \to 0$). For increasing γ_2 the squeezing in the output of the waveguide ($M1$) is reduced, whereas the squeezing at the mirror $M2$ output is enhanced. In this case there are two independent inputs which cannot interfere to cancel the fluctuations and increase the squeezing in the quadrature.

As outlined in the stability analysis, additional losses are generated by the feedback in the case of constructive interference, and thereby the system remains stable. The spectrum is broadened around ω_0 so that the squeezing is maximal over a large frequency region. In the lossless case ($\gamma_2 = 0$, not shown here) we find perfect squeezing at the threshold curve (boundary between stable and unstable region). Furthermore, we observe a frequency region of constant squeezing in the spectrum for stable points in the short delay regime as P [cf. Fig. 2(a)]. On the other hand, when passing the border between the short- and long-delay regimes, the spectra have a dip at ω_0 (not shown) which grows with the value of the feedback coupling strength γ_1.

VII. CONCLUSION

We have shown how quantum coherent time-delayed feedback of Pyragas type [3] can be used to control and enhance the squeezing performance at the output of a cavity containing a degenerate parametric oscillator. We proposed two physically different setups to introduce feedback. Both could be modeled on equal footing. Our main result is that coherent feedback causes a frequency-dependent modification of the power spectral density of the output field quadratures, compared to the uncontrolled case. For the application of control, the Lorentzian form of the uncontrolled squeezing spectrum becomes sharply multipeaked due to frequency-dependent interferences within the feedback loop. In particular, we find a strong enhancement of squeezing for specific delay times. A thorough stability analysis shows that in the case of constructively interfering signals within the feedback loop, new loss channels are created, meaning that the pump intensity of the laser can be increased while the system remains stable. This becomes particularly important in the short-delay regime as this allows enhancement of the squeezing in one of the system's output channels far below the quantum noise limit.

Note added. Recently we became aware that a closely related work was posted on Ref. [45].

ACKNOWLEDGMENTS

We thank Alexander Carmele for very helpful discussions. We acknowledge support from Deutsche Forschungsgemeinschaft (DFG) through SFB 910 "Control of self-organizing nonlinear systems" (Project B1 and Project A1). Also, discussions with our colleagues involved in Project A7 are acknowledged. S.H. acknowledges funding from the Natural Sciences and Engineering Research Council of Canada (NSERC).

APPENDIX: DESCRIPTION OF QUANTUM-COHERENT TIME-DELAYED FEEDBACK

In this Appendix we present a method to describe quantum coherent time-delayed feedback using the input-output theory [24,30]. Starting from the well-known description of quantum cascaded systems, we will show how the formalism can be used to describe quantum coherent feedback, where previous versions of the system drive the present one. Note that the input-output theory uses a Markov approximation that is only valid for a weak system-reservoir coupling. Therefore, it is important to ensure that the feedback setup does not alter the coupling of the system to a continuum of reservoir modes. A principal difficulty lies in the fact that no master equation exists since the system becomes highly non-Markovian in the presence of feedback. An attempt following the precedent idea to solve the nonlinear system by embedding the feedback system in a larger space is found in Ref. [23]. Also Pyragas-type feedback control schemes can be realized where the system is driven towards a desired steady state [8].

1. Coherent feedback as a quantum cascaded system

In what follows we want to investigate the problem of a system driven coherently by a past version of itself. We shall use the input-output theory applied to cascaded systems [24,30].

To begin, let us consider the textbook case of a bipartite quantum system with total Hamiltonian H_{sys} that can be decomposed into two subsystems A and B with Hamiltonian H_A and H_B respectively. We will later modify the system such that it represents time-delayed self-feedback. The total system is interacting with the modes of an external reservoir with Hamiltonian $H^1_R = \hbar \int_{-\infty}^{\infty} d\omega\, \omega b^\dagger(\omega) b(\omega)$, where $b^{(\dagger)}(\omega)$ are bosonic field modes satisfying $[b(\omega), b^\dagger(\omega')] = \delta(\omega - \omega')$. The systems A and B interact with the reservoir through their respective operators c_A and c_B.

In terms of the input-output theory, we now drive the input of the first system A with the bosonic field induced by the external reservoir modes. The interaction Hamiltonian of A with the reservoir is therefore (within the rotating-wave approximation)

$$H_{\text{Int},1} = i\hbar\sqrt{\frac{\gamma_1}{2\pi}} \int_{-\infty}^{\infty} d\omega\, [b^\dagger(\omega) c_A - \text{H.c.}]. \tag{A1}$$

Furthermore we assume that the second system B is driven by the time-delayed and phase-shifted output field of the first

one so that the interaction Hamiltonian takes the form

$$H_{\mathrm{Int},2} = i\hbar\sqrt{\frac{\gamma_f}{2\pi}}\int_{-\infty}^{\infty} d\omega\,[b^\dagger(\omega)e^{i\omega\tau}e^{i\phi}c_B - \mathrm{H.c.}], \quad \text{(A2)}$$

where γ_1 and γ_f are the coupling elements, which are constant. This is the result of a standard approximation often called the first Markov approximation [24], which holds true when all coupling from the system to the reservoir is within a narrow bandwidth of frequency [30]. The term $\omega\tau$ is such that τc_0 is the distance between the two systems, with c_0 being the speed of light. Furthermore, we consider an additional phase-shift ϕ of the field, which may be induced by an external boundary condition, e.g., by a mirror. The f in the coupling constant γ_f stands for feedback and points out that the system B is coupled to the time-delayed light field emitted by A. We extend the treatment by additionally coupling A to another reservoir H_R^k, $k \in \{2,3,\dots\}$ independent of H_B^1 in the form (A1). We distinguish the reservoirs via the superscript in H_R^k. Figure 6 shows schematically the cascaded system. From the standard input-output theory we derive the following Langevin equation for an arbitrary operator X of the systems A or B [46]:

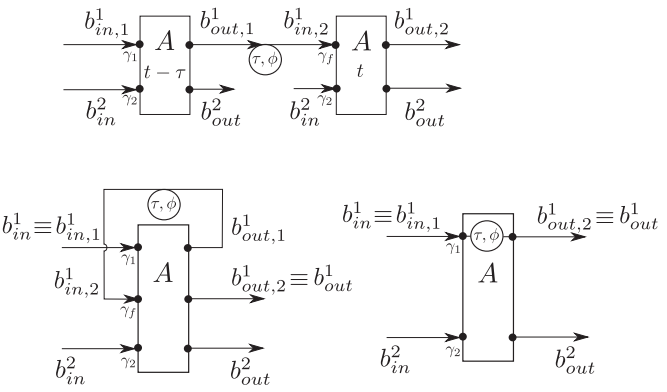

FIG. 6. Our feedback scheme. Top: A system is coherently driven in a cascaded fashion by a past version of itself via the feedback in-loop field $b^1_{\mathrm{in},2}(t) = e^{i\phi}b^1_{\mathrm{out},1}(t-\tau)$. The additional input b^2_{in} takes account of additional drives or losses of the system independent of b^1_{in}. Left bottom: Same physical setup represented by a loop. Right bottom: The in-loop field can be eliminated; its only purpose is to modify the internal dynamic. Note that b^1_{out} never influences the system again.

$$\dot{X} = -\frac{i}{\hbar}[X, H_A + H_B] \quad \text{(A3a)}$$

$$-\sum_k \left\{[X, c_A^\dagger]\left(\frac{\gamma_k}{2}c_A + \sqrt{\gamma_k}b^k_{\mathrm{in}}(t)\right) - \left(\frac{\gamma_k}{2}c_A^\dagger + \sqrt{\gamma_k}b^{k\dagger}_{\mathrm{in}}(t)\right)[X, c_A]\right\} \quad \text{(A3b)}$$

$$-[X, c_B^\dagger]\left(\frac{\gamma_f}{2}c_B + \sqrt{\gamma_1\gamma_f}c_A(t-\tau)\,e^{i\phi} + \sqrt{\gamma_f}b^1_{\mathrm{in}}(t-\tau)\,e^{i\phi}\right)$$

$$+\left(\frac{\gamma_f}{2}c_B^\dagger + \sqrt{\gamma_1\gamma_f}c_A^\dagger(t-\tau)\,e^{-i\phi} + \sqrt{\gamma_f}b^{1\dagger}_{\mathrm{in}}(t-\tau)\,e^{-i\phi}\right)[X, c_B]. \quad \text{(A3c)}$$

We have defined the input operator $b^k_{\mathrm{in}}(t) = 1/\sqrt{2\pi}\int_{-\infty}^{\infty} d\omega\, b^k_0(\omega)e^{-i\omega t}$, which only depends on the initial reservoir operator $b^k_{t=0}(\omega)$.

We see from Eq. (A3) that only system A has an effect on system B, whereas B does not influence A. Thus we have an unidirectional coupling field from A to B.

This setup can now be modified to represent time-delayed feedback: In the following we consider only one additional reservoir H_R^2 beside H_R^1. To describe a system driven coherently by a past version of itself through a feedback channel, we now go one step further and let the two subsystems H_A and H_B become the same system H_{sys}, which means that $c_A = c_B = c$. We consider the equation of motion for the operator c, which from (A3) takes the form

$$\dot{c} = -\frac{i}{\hbar}[c, H_{\mathrm{sys}}] - \frac{\gamma_1+\gamma_2+\gamma_f}{2}c(t) - \sqrt{\gamma_1\gamma_f}e^{i\phi}c(t-\tau)$$
$$-\sqrt{\gamma_1}b^1_{\mathrm{in}}(t) - \sqrt{\gamma_2}b^2_{\mathrm{in}}(t) - \sqrt{\gamma_f}e^{i\phi}b^1_{\mathrm{in}}(t-\tau). \quad \text{(A4)}$$

Equation (A4) is a time-delayed differential equation. This is a quite general equation; indeed no assumptions have yet been made about the system Hamiltonian nor the initial statistics of the reservoir. The input operators b_{in} only depend on the initial condition b_0. They can therefore be interpreted as noise terms if the system and reservoir are initially factorized and b_0 is in an incoherent state. The delayed term $b^1_{\mathrm{in}}(t-\tau)$ indicates that past fluctuations have an influence on the dynamics of the present system. We now simply have the situation of a system interacting with an input field giving rise to an output field which interacts with the system again after a delay τ and a phase shift ϕ. Moreover, causality has to be preserved, which means that the system at later times should not influence the previous system. This is naturally ensured in the present case, where sys_1 (previous) influences sys_2 (later) but the reverse direction is forbidden. Therefore, the input-output theory for quantum cascade systems is well suited for the treatment of a quantum coherent description of autonomous time-delayed feedback as it allows input to output connections with preservation of causality. A graphical representation of the cascade is given in Fig. 6 (top).

2. Description of feedback in terms of loops

We define output fields related by the standard input-output relation [30]

$$b^k_{\mathrm{out},\alpha}(t) = b^k_{\mathrm{in},\alpha}(t) + \sqrt{\gamma_{k,\alpha}}\,c(t). \quad \text{(A5)}$$

The subscript α labels the input and output ports, which are driven by fields from the same reservoir k. The problem is schematically shown in Fig. 6 (bottom left). We omit the subscript in the case where the operator $b^k_{\text{in/out}}$ only acts on one port of the system.

We remark that (A4) can be directly obtained by coupling the system to two bosonic fields $b^1_{\text{in},1}(t)$ and $b^1_{\text{in},2}(t)$ with respective strength γ_1 and γ_f by letting

$$b^1_{\text{in},2}(t) = e^{i\phi} b^1_{\text{out},1}(t-\tau). \tag{A6}$$

Using the input-output relation (A5) we can directly connect the in-loop input to the free input b^1_{in}, that is,

$$b^1_{\text{in},2}(t) = e^{i\phi}\left[b^1_{\text{in},1}(t-\tau) + \sqrt{\gamma_1}c(t-\tau)\right]. \tag{A7}$$

Inserting the new input $b^1_{\text{in},2}$ in (A3) without (A3c) reproduces (A4).

This is an interesting point since it gives an intuitive picture of autonomous feedback. In fact the field b^1_{in} induced by the reservoir gives rise to the in-loop field $b^1_{\text{out},1}$. This is propagating back into the system again to become the input $b^1_{\text{in},2}$ after having experienced a phase shift ϕ and a delay time τ. The only purpose of this in-loop field is to modify the internal dynamics of the system and may then be lost in form of the output $b^1_{\text{out},2}$. That means that the information of the past system is only stored for the duration of one loop in the feedback channel and may then be forgotten. Therefore, only one τ appears in the equation.

In the present case we do not allow $b^1_{\text{out},2}$ to influence the system again, but we can straightforwardly extend Eq. (A4) to include this case. However, the present treatment is sufficient for a number of problems dealing with time-delayed feedback in open quantum systems when the coupling between system and reservoir is weak; see, e.g., Refs. [7,8,12]. We will discuss that in the next section.

3. Equivalence of the proposed coherent feedback scheme to other approaches

We reconsider now the Hamiltonians of Sec. (A 1). We will show that our coherent feedback scheme is equivalent to other approaches found in the literature.

Consider the case where the interactions $H_{\text{int},1}$ and $H_{\text{int},2}$ of the system with the reservoir H^1_R are done with the same operator $c_A = c_B = c$ and are of same strength, that is, $\gamma_1 = \gamma_f$. Furthermore, consider a phase shift $\phi = \pi$.

We introduce the interaction Hamiltonian H_{int} as the sum of $H_{\text{int},1}$ and $H_{\text{int},2}$:

$$\begin{aligned} H_{\text{int}} &= H_{\text{int},1} + H_{\text{int},2} \\ &= 2\hbar\sqrt{\frac{\gamma_1}{2\pi}}\int_{-\infty}^{\infty} d\omega\,[\sin(\omega\tau/2)B^\dagger(\omega)c + \text{H.c.}]. \end{aligned} \tag{A8}$$

Here we have defined the new bosonic operator

$$B(\omega) = e^{-i\omega\tau/2}b(\omega). \tag{A9}$$

This is exactly the interaction Hamiltonian found when coupling a system weakly to an external continuum of modes shaped by a mirror, as is done, e.g., in Refs. [7,12,47].

Since $H^1_R = \hbar\int d\omega\,\omega b^\dagger(\omega)b(\omega) = \hbar\int d\omega\,\omega B^\dagger(\omega)B(\omega)$, the system dynamics described by the total Hamiltonian $H = H_{\text{sys}} + H^1_R + H_{\text{int}}$ is therefore totally equivalent in the two approaches. The input-output theory as already outlined before particularly gives a more intuitive picture of the feedback problem.

4. Eliminating the in-loop field

It should be mentioned that it is impossible to measure the in-loop field without destroying the quantum coherence of the feedback loop, so that the only purpose of this field is to modify the internal dynamics. It is suitable to derive a direct relation between the free output $b^1_{\text{out},2} \equiv b^1_{\text{out}}$ to the free input b^1_{in} since it avoids dealing with nonstandard commutation relation as (A17) when considering, e.g., correlations of the inputs. This is easily done using the input-output relation. We have

$$b^1_{\text{out}}(t) = e^{i\phi}b^1_{\text{in}}(t-\tau) + e^{i\phi}\sqrt{\gamma_1}c(t-\tau) + \sqrt{\gamma_f}c(t). \tag{A10}$$

A graphical representation is given by Fig. 6 (right bottom). In the main part of the paper a Fourier representation of Eq. (A10) is needed. Using the Fourier transformed field operators defined by

$$\tilde{O}(w) = \frac{1}{\sqrt{2\pi}}\int_{-\infty}^{\infty} dt\, e^{-i\omega t}O(t), \tag{A11}$$

we can transform (A10) into

$$\tilde{b}^1_{\text{out}}(\omega) = e^{i\phi}e^{-i\omega\tau}\tilde{b}^1_{\text{in}}(\omega) + (\sqrt{\gamma_1}e^{i\phi}e^{-i\omega\tau} + \sqrt{\gamma_f})\tilde{c}(\omega). \tag{A12}$$

In the same way, the input-output relation for $b^2_{\text{in}}/b^2_{\text{out}}$, $b^2_{\text{out}}(t) = b^2_{\text{in}} + \sqrt{\gamma_2}c(t)$, is simply

$$\tilde{b}^2_{\text{out}}(\omega) = \tilde{b}^2_{\text{in}}(\omega) + \sqrt{\gamma_2}\tilde{c}(\omega). \tag{A13}$$

In a general form, covering both relations, we can write Eqs. (A12) and (A13) as

$$\tilde{b}^i_{\text{out}}(\omega) = X_i(\omega)\tilde{b}^i_{\text{in}}(\omega) + Y_i(\omega)\tilde{c}(\omega), \tag{A14}$$

where X_i and Y_i are defined in Eqs. (A12) and (A13) and are used as an abbreviation in the main part of the paper.

5. Commutator relations

The input fields b^i_{in} obey the bosonic commutator relation

$$\left[b^i_{\text{in}}(t), b^{j\dagger}_{\text{in}}(t')\right] = \delta_{ij}\delta(t-t'), \tag{A15}$$

and in the case of a vacuum input, the only nonvanishing correlation is

$$\left\langle b^i_{\text{in}}(t)b^{i\dagger}_{\text{in}}(t')\right\rangle = \delta(t-t'). \tag{A16}$$

For the in-loop input $b^1_{\text{in},2}$ this relation are modified since $b^1_{\text{in},2}$ is not independent of b^1_{in} and the system operator c. We have for the commutator

$$\left[b^1_{\text{in},2}(t), b^{1\dagger}_{\text{in},2}(t')\right] = \delta(t-t') \quad \text{for} \quad |t-t'| < \tau, \tag{A17}$$

which can be found using Eqs. (A5) and (A6) and for reasons of causality $[b^{1(\dagger)}_{\text{out},1}(t'), c^{(\dagger)}(t)] = 0$ for $t - t' < \tau$ (see, e.g., Ref. [30]).

Thus the in-loop field obeys the canonical commutator relation only for $|t-t'| < \tau$ but not for time differences greater than the loop time.

Ensuring that the time difference $|t - t'|$ is less than the delay τ guarantees that the two-time commutator remains canonical as it evaluates between fields in coexistence in the loop.

6. Pyragas-type quantum control scheme

If we consider the situation where the phase shift is $\phi = \pi$ and the coupling is $\gamma_1 = \gamma_f = \gamma$ (perfect coupling) and $\gamma_2 = 0$ (lossless) the feedback channel *engineers* a quantum control scheme, which is of Pyragas type [3]. In this scheme Eq. (A4) becomes

$$\dot{c} = -\frac{i}{\hbar}[c, H_{\rm sys}] - \gamma_1[c(t) - c(t-\tau)] - \sqrt{\gamma_1}b^1_{\rm in}(t) + \sqrt{\gamma_1}b^1_{\rm in}(t-\tau). \tag{A18}$$

In this scheme the term $\gamma_1[c(t) - c(t-\tau)]$ acts as a control force and vanishes in case of stabilization, when the system reaches a steady state or is τ periodic, i.e., if $c(t) = c(t-\tau)$. The output field is then, using (A10), $b^1_{\rm out}(t) = -b^1_{\rm in}(t-\tau) + \sqrt{\gamma_1}[c(t) - c(t-\tau)]$. When the system reaches a steady state we will have $c(t) = c(t-\tau)$ and in consequence the system operator will be stabilized. For the output field we then have $b^1_{\rm out}(t) = -b^1_{\rm in}(t-\tau)$. That means only noise remains as an output in case of stabilization. The Pyragas scheme is noninvasive since the control force vanishes in the case of stabilization. Pyragas-type stabilization schemes have been used in coherent feedback control, e.g., to reach fast steady-state convergence in open quantum systems [8]. We presented recently how to use a Pyragas scheme to control entanglement in a quantum node network [9].

[1] S. Lloyd, Phys. Rev. A **62**, 022108 (2000).
[2] A. Serafini, ISRN Optics **2012**, 275016 (2012).
[3] K. Pyragas, Phys. Lett. A **170**, 421 (1992).
[4] P. Hövel and E. Schöll, Phys. Rev. E **72**, 046203 (2005).
[5] E. Schöll and H. G. Schuster, eds., *Handbook of Chaos Control* (Wiley-VCH, Weinheim, Germany, 2008).
[6] C. Grebogi, *Recent Progress in Controlling Chaos,* Series on Stability, Vibration, and Control of Systems (World Scientific, Singapore, 2010).
[7] A. Carmele, J. Kabuss, F. Schulze, S. Reitzenstein, and A. Knorr, Phys. Rev. Lett. **110**, 013601 (2013).
[8] A. L. Grimsmo, A. S. Parkins, and B.-S. Skagerstam, New J. Phys. **16**, 065004 (2014).
[9] S. M. Hein, F. Schulze, A. Carmele, and A. Knorr, Phys. Rev. A **91**, 052321 (2015).
[10] H. Pichler and P. Zoller, Phys. Rev. Lett. **116**, 093601 (2016).
[11] I.-C. Hoi, A. F. Kockum, L. Tornberg, A. Pourkabirian, G. Johansson, P. Delsing, and C. M. Wilson, Nat. Phys. **11**, 1045 (2015).
[12] U. Dorner and P. Zoller, Phys. Rev. A **66**, 023816 (2002).
[13] H. J. Carmichael, *Statistical Methods in Quantum Optics 2: Non-Classical Fields* (Springer, Berlin, 2008).
[14] H. J. Carmichael, Proc. SPIE **5111**, 301 (2003).
[15] T. C. Ralph, in *Quantum Information with Continuous Variables* (Springer, Dordrecht, 2003), p. 295.
[16] V. M. Bastidas, I. Omelchenko, A. Zakharova, E. Schöll, and T. Brandes, Phys. Rev. E **92**, 062924 (2015).
[17] H. M. Wiseman, M. S. Taubman, and H.-A. Bachor, Phys. Rev. A **51**, 3227 (1995).
[18] H. M. Wiseman and G. J. Milburn, *Quantum Measurement and Control* (Cambridge University Press, Cambridge, UK, 2009).
[19] J. E. Gough and S. Wildfeuer, Phys. Rev. A **80**, 042107 (2009).
[20] J. E. Gough, M. R. James, and H. I. Nurdin, Phys. Rev. A **81**, 023804 (2010).
[21] O. Crisafulli, N. Tezak, D. B. S. Soh, M. A. Armen, and H. Mabuchi, Opt. Express **21**, 18371 (2013).
[22] S. Iida, M. Yukawa, H. Yonezawa, N. Yamamoto, and A. Furusawa, IEEE Trans. Autom. Control **57**, 2045 (2012).
[23] A. L. Grimsmo, Phys. Rev. Lett. **115**, 060402 (2015).
[24] C. W. Gardiner and M. J. Collett, Phys. Rev. A **31**, 3761 (1985).
[25] P. Yao and S. Hughes, Phys. Rev. B **80**, 165128 (2009).
[26] V. S. C. M. Rao and S. Hughes, Phys. Rev. Lett. **99**, 193901 (2007).
[27] S. Hughes, Phys. Rev. Lett. **98**, 083603 (2007).
[28] J.-T. Shen and S. Fan, Phys. Rev. A **79**, 023837 (2009).
[29] M. J. Collett and C. W. Gardiner, Phys. Rev. A **30**, 1386 (1984).
[30] C. W. Gardiner and P. Zoller, *Quantum Noise* (Springer, New York, 2010).
[31] T. Kamalakis and T. Sphicopoulos, IEEE J. Quantum Electron. **41**, 1419 (2005).
[32] K. Koshino and Y. Nakamura, New J. Phys. **14**, 043005 (2012).
[33] M. Bradford and J.-T. Shen, Phys. Rev. A **87**, 063830 (2013).
[34] G. Hétet, L. Slodička, M. Hennrich, and R. Blatt, Phys. Rev. Lett. **107**, 133002 (2011).
[35] J. Eschner, C. Raab, F. Schmidt-Kaler, and R. Blatt, Nature (London) **413**, 495 (2001).
[36] R. Lang and K. Kobayashi, IEEE J. Quantum Electron. **16**, 347 (1980).
[37] F. Schulze, B. Lingnau, S. M. Hein, A. Carmele, E. Schöll, K. Lüdge, and A. Knorr, Phys. Rev. A **89**, 041801 (2014).
[38] C. Diederichs, J. Tignon, G. Dasbach, C. Ciuti, A. Lemaitre, J. Bloch, P. Roussignol, and C. Delalande, Nature (London) **440**, 904 (2006).
[39] C. Reimer, M. Kues, L. Caspani, B. Wetzel, P. Roztocki, M. Clerici, Y. Jestin, M. Ferrera, M. Peccianti, A. Pasquazi *et al.*, Nat. Commun. **6**, 8236 (2015).
[40] A. Thowsen, Int. J. Control **33**, 991 (1981).
[41] H. Shinozaki, Ph.D. thesis, Kyoto Institute of Technology, 2007.
[42] E. M. Wright, Proc. Royal Soc. Edinburgh, Sec. A **62**, 387 (1949).
[43] A. Amann, E. Schöll, and W. Just, Phys. A (Amsterdam, Neth.) **373**, 191 (2007).
[44] Although our scheme involves a double-sided cavity, for destructive interference it shows the squeezing performance of a single-ended cavity pumped at threshold without feedback [29].
[45] N. Német and S. Parkins, arXiv:1606.00178.
[46] C. W. Gardiner, Phys. Rev. Lett. **70**, 2269 (1993).
[47] S. M. Hein, F. Schulze, A. Carmele, and A. Knorr, Phys. Rev. Lett. **113**, 027401 (2014).